

## Preparation of a Superhydrophobic Film with UV Imprinting Technology

Young-Wook Choi\*

Display Material Division, Cheil Industries Inc, Euiwang 437-010, Korea

Jung-Eun Han

R & D Center, LG Micron, Ansan 426-791, Korea

Songyi Lee and Daewon Sohn

Department of Chemistry & Research Institute for Natural Science, Hanyang University, Seoul 133-791, Korea

Received January 30, 2009; Revised March 8, 2009;

Accepted March 23, 2009

### Introduction

Superhydrophobic surfaces with an advancing water contact angle (CA) larger than  $150^\circ$  and a water sliding angle (SA) less than  $10^\circ$  are found on lotus leaves and butterfly wings. These surfaces are interesting because of their various applications for water-repellence and anti-sticking properties.<sup>1,2</sup> The lotus leaf is especially well known for its self-cleaning ability. Rolling water droplets wash off contaminants and dust due to low surface adhesion. According to previous studies,<sup>1,2</sup> the surface dewetting is governed by the surface energy of coating material and roughness of the surface. Poly(dimethylsiloxane) (PDMS) and fluorocarbon based materials have been used to artificially modify a surface due to their low surface free energies.<sup>3-6</sup> Nanotubes, nanofibers, nanorods, and porous structures<sup>7-11</sup> have been introduced to create complex nano structures.

Theoretically, two distinct models (Wenzel and Cassie models<sup>12,13</sup>) were proposed to explain the effect of roughness on a hydrophobic surface. Because roughness impacts contact angles, they introduced the surface roughness factor ( $r$ ), which is defined as the ratio between the actual and projected surface areas. Wenzel derived a theoretical relationship from the Young equation, which correlates the 'apparent' or measured contact angle on a rough surface with a flat substrate (Young's model). His equation shows that an increased  $r$  can enhance surface wettability, allowing water to penetrate the surface. Cassie and Baxter, on the other hand, propose that an  $r$  above a critical level leads to a great decrease in CA hysteresis, therefore increasing the receding angle. In the Cassie model, water droplets partially sit on surface air

pockets and can easily roll off.

In the previous study, we showed a simple method to imitate the hierarchical lotus leaf structure using sol-gel technology. Briefly, we used a micro lens array (MLA) pattern to create ordered, micron-sized, large hills and porous silica aerogel to create disordered nano structure, and then chemically modified the surface with a PDMS coating solution.<sup>14</sup>

Nano-imprint lithography (NIL) is a promising technique to fabricate patterned structures with high precision and throughput in the micro/nanometer scale region. Additionally, NIL is inexpensive and does not require a complicated apparatus.<sup>15,16</sup> In conventional NIL technology, hard molds, such as silicon, dielectric material (e.g., silicon dioxide or silicon nitride), and metal material (e.g., nickel) were used.<sup>17</sup> Recently, flexible mold technology was introduced, replacing hard molds, making it easier to release the mold from the polymer surface, providing better conformal contact with the substrate to be patterned, and reducing the pressure needed during imprinting.<sup>18-20</sup> In a previous study, Kim *et al.* introduced a simple NIL method to create a superhydrophobic surface with a flexible mold made from anodic aluminium oxides (AAOs).<sup>21</sup> Furthermore, Lee *et al.* produced well-defined, large, nanostructured polymeric and metallic surfaces with nanoembossing or nanofibers and controlled aspect ratios by employing AAOs or textured Al surfaces as a replication master.<sup>22</sup>

In this study, we present a superhydrophobic flexible film preparation with ultraviolet (UV) NIL technology using a flexible master substrate with ordered micron-sized patterns and disordered nano structure. The advantage of this study is that it removes the surface treatment step that is required in conventional imprinting. The surface treatment allows for easy demolding due to the low surface energy of the superhydrophobic and modified-PDMS coating surface.

### Experimental

**Material.** A large MLA sheet (120 cm  $\times$  120 cm) for the display device was kindly donated by LG Micron. The MLA sheet was prepared by micro-replication. Silicon coating solution (1-2577) was purchased from Dow Corning and used without further purification. The original coating solution consists of 60% dimethyl methylphenylmethoxy siloxane, 30% toluene, and 10% methyltrimethoxysilane. Aerosol silica particles (Micloid, ML381) were purchased from Dongyang Chemical, Co. The advertised average particle size is about 1-5  $\mu\text{m}$  and the particle porosity was  $\sim 1.5$  mL/g, as determined by the BET method. Norland Optical adhesives (NOA 63), a mercapto ester-type UV curable prepolymer was purchased from Norland Company.

\*Corresponding Author. E-mail: youngwook.choi@samsung.com

**Coating.** 30 g toluene was added to 70 g of original silicon solution to adjust viscosity of coating solution. 1 g silica powder was then poured into 9 g diluted coating solution. The final silica concentration was 10% by wt. The mixed solution was stirred for 24 h.

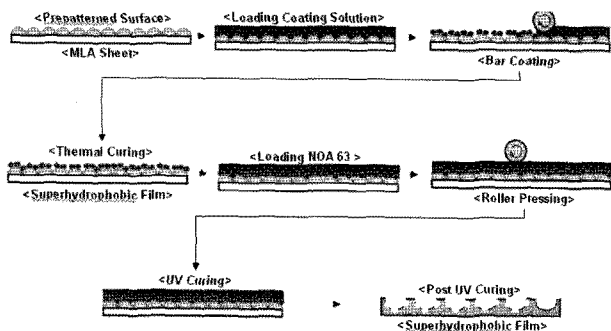
**Imprinting.** A flexible polymer mold was fabricated on a PET substrate as shown in Scheme I. The mold dispensed with NOA 63 was pressed with PET and the assembly was polymerized under UV lamps for 10 min. After peeling off, the mold was post-cured for 30 min.

**Characterization.** All images were obtained using a field emission scanning microscope (FE-SEM) (Nova nanolab, FEI), operated at 10 kV. We used the SEO contact angle analyzer (Surface Electro Optics, Phoenix) to measure the static and dynamic contact angles. Static contact angles were measured by the sessile drop method and reported values are the average of five measurements. The sliding angle measurement was performed with a lab-made sliding angle measuring system. All angles were measured at ambient temperature.

## Results and Discussion

A polymer mold material for imprinting technology should have a high modulus to withstand deformation during imprinting. A commercial UV-curable polymer (Norland Optical Adhesive (NOA) 63, Norland Products Inc.) is suitable for nanometer-scale contact printing and imprint lithography because NOA 63 has a modulus of 1,655 MPa. Furthermore, the fabricated mold is highly flexible owing to the poly(ethylene terephthalate) (PET) backplane that supports the NOA 63 nano-features. Hammond *et al.* showed that NOA 63 can replicate 80 nm features by contact printing.<sup>18-20</sup> Therefore, we used NOA 63 for the hard replication film and a hard template as a son mold.

Scheme I shows the fabrication procedure for a negatively replicated polymer film with a flexible master template that has a hierarchically distributed micro/nano pattern structure. As mentioned in a previous study, the mother mold was



**Scheme I.** Schematic illustration of the preparation of honeycomb-like superhydrophobic film using a flexible primary mold. The supported substrate is PET film at each step.

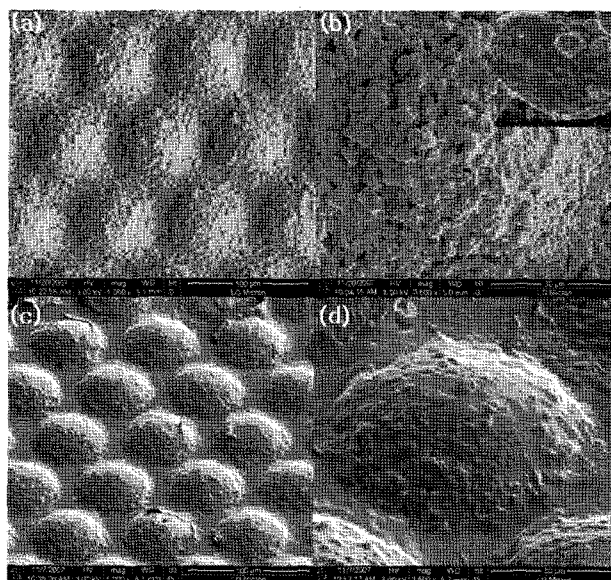


**Figure 1.** SEM images of MLA patterns coated with porous silica particles: (a) large area figure; (b) top view of close figure with single lens; (c) deformed large area figure after imprinting; (d) top view of close figure of deformed single lens. Inset of Figure 1(b) well shows nano-protrusion of coated large hill.

generated by bar coating with a mixed solution consisting of porous silica particles and a PDMS modified solution with 50 micrometer MLA pattern substrates.

The scanning electron microscope (SEM) images in Figures 1(a) and 1(b) show well-generated hierarchical micro/nano surface structure. The static water CA of the prepared primary mold was about  $155 \pm 2^\circ$  and the sliding angle (SA) was about  $4 \pm 1^\circ$ , with no pinned-on points in the large area.

Typically, the nano-imprint lithography mold has a large number of nano-meter scale extrusion/intrusion features on its surface. These intrusions significantly increase the total surface area contacting the imprinted polymer, leading to strong adhesion between the imprinted polymer and mold. The most common method is to form a self-assembled mono-layer of fluorosilane release agent on the mold surface from solution or vapour phase, or to apply a low surface energy coating to the mold.<sup>23,24</sup> There is no anti-adhesion surface treatment step of our flexible master template because the low-surface energies of both the PDMS coat and superhydrophobic surface act as an anti-adhesion layer.

The UV curable resin (NOA 63) with a PET flexible film was printed on the hierarchical structure mold. The cylindrical roller was then used to uniformly coat the mold with substrate and prevent the formation of unpatterned regions due to trapped air. After curing with UV light for 10 min, the NOA 63 replica film was easily peeled off the mold. The negative film was post-cured for 30 min with UV light. The primary superhydrophobic mold was reused several

times. One disadvantage of reusing the mold is deformation of nano extrusion structure on the primary template. The master was deformed after 5-10 uses due to a relative low general PDMS film modulus (2.4-4.5 MPa). The SEM images in Figures 1(a) and 1(c) show the surface before and after imprinting. As shown in Figure 1(c), the coating surface gets stripped off. A nano-protrusion feature (the top of a large hill) was severely collapsed after 5-10 repetitions. As a result of decreased surface roughness, the water CA decreased from  $155 \pm 2^\circ$  to  $130 \pm 5^\circ$ .

Figure 2 shows an SEM image of a flexible negative film replicated from a positive superhydrophobic master. Figure 2(a) shows a  $45^\circ$  tilted large area SEM clearly showing the inverse features of the original template. The top-view of the negative film exhibits a honeycomb-like texture with sharp edges and surface pores. The inverse pattern has an ordered micro porous pattern and a randomly distributed sink nano structure. Figure 2(c) shows a fine nano-intrusion feature that is mimicked by extrusion of a primary mold. The another evidence of transferability from mother to son mold of unregular pattern is the quantitative analysis on the basis of the AFM images although it is hard to compare good transferability with roughness factor. The root-mean-square roughness ( $R_q$ ) is  $900 \pm 14$  nm with projected patterns and the  $R_q$  is  $1,000 \pm 30$  nm with collapsed structures. These figures demonstrate the ability of NOA 63 to transfer nano pattern structures with a high accuracy.

Our honeycomb-like feature showed very similar morphology to the superhydrophobic surface made by the Rubner group.<sup>25</sup> His group created a honeycomb-like structure

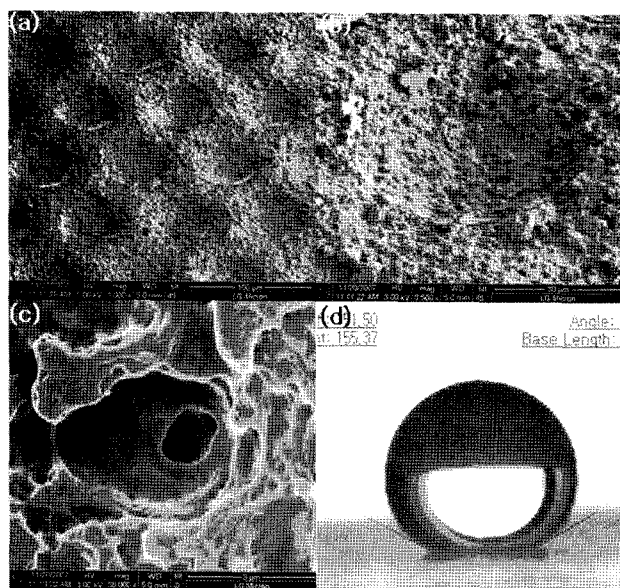


**Figure 2.** SEM images of replicated negative patterns imprinted with NOA 63: (a) tilted large area figure; (b) top view of close figure with single lens; (c) magnified nano-sink feature of negative film; (d) the water contact angle of imprinted pattern.

using a polyelectrolyte multilayer surface overcoated with silica nanoparticles. Therefore, the static CA and sliding angle were measured with this pattern to investigate the hydrophobicity of the inverse mold. Although we know the importance of reporting the advancing and receding CAs,<sup>26</sup> measuring both CA angles due to water-repellence of the surface was very difficult. Because of these experimental problems, we report the sliding angles, which are related to the contact angle hysteresis.<sup>27</sup> Figure 2(d) shows the static CA on the replicated surface. The static CA measured by the sessile drop method was  $152 \pm 2^\circ$  and the sliding angle measured with a home-made tilting device was  $6 \pm 2^\circ$ .

In general, self-cleaning and dust-free surfaces are very useful on glass for display and optical applications. The micro porous superhydrophobic morphology was imprinted on glass to show that imprinting can provide unusual wetting to any surface, provided the surface can adhere to NOA 63.

To show the self-cleaning effect of the imprinted pattern on glass, we sprayed black carbon powders on the surface. Figure 3 clearly shows that the superhydrophobic surface self-cleans. When several water droplets were washed across the surface, the contaminant was easily removed by rolling water drops due to stronger adhesion to the water drop than the surface. The arrow in Figure 3 shows the direction of a water drop from (1), which is a mopped surface to (2), which is polluted surface.

In summary, we introduced a simple preparation of a negative replication film with room-temperature UV-NIL technique using a flexible superhydrophobic coating mold without additional anti-adhesion treatment. The honeycomb-like structure, that is an inverse imitation of the master, showed good superhydrophobic properties. The sol-gel coating on a patterned structure can enable manufacturing of a large area template and this imprinting technique can allow for mass production.

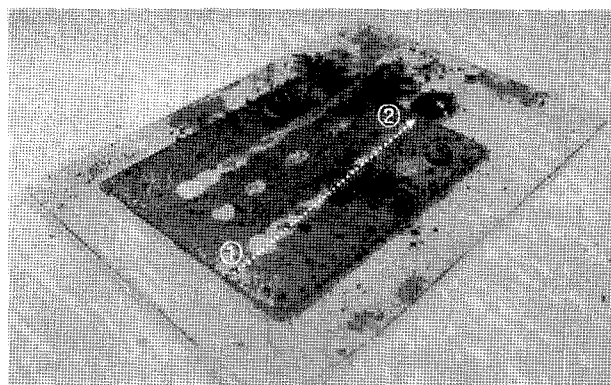


**Figure 3.** Demonstration of self-cleaning effect by rolling a water drop to remove the carbon black powder. An arrow shows the trace of a rolling water droplet.

**Acknowledgments.** This work has been supported by the research fund of Hanyang University 2007.

## References

- (1) C. Neinhuis and W. Barthlott, *Ann. Bot.*, **79**, 667 (1997).
- (2) W. Barthlott and C. Neinhuis, *Planta*, **202**, 1 (1997).
- (3) J. L. Zhang, J. A. Li, and Y. C. Han, *Macromol. Rapid Commun.*, **25**, 1105 (2004).
- (4) A. Singh, L. Steely, and H. R. Allcock, *Langmuir*, **21**, 11604 (2005).
- (5) W. Ming, D. Wu, R. van Benthem, and G. de Width, *Nano Lett.*, **5**, 2298 (2005).
- (6) G. R. J. Artus, S. Jung, J. Zimmermann, K. Marquardt, and S. Seeger, *Adv. Mater.*, **18**, 2758 (2006).
- (7) L. Feng, S. Li, Y. Li, H. Li, L. Zhang, Y. Song, B. Liu, L. Jiang, and D. Zhu, *Adv. Mater.*, **14**, 1857 (2002).
- (8) T. Sun, L. Feng, X. Gao, and L. Jiang, *Acc. Chem. Res.*, **38**, 644 (2005).
- (9) E. Hosono, S. Fujihara, I. Honma, and H. Zhou, *J. Am. Chem. Soc.*, **127**, 13458 (2005).
- (10) G. Zhang, D. Wang, Z.-Z. Gu, and H. Mohwald, *Langmuir*, **21**, 9143 (2005).
- (11) A. Nakajima, A. Fujishima, K. Hashimoto, and T. Watanabe, *Adv. Mater.*, **11**, 1365 (1999).
- (12) R. N. Wenzel, *Ind. Eng. Chem.*, **28**, 998 (1936).
- (13) B. D. Cassie and S. Baxter, *Trans. Faraday Soc.*, **40**, 546 (1944).
- (14) Y.-W. Choi, J. Han, S. Eom, Y. S. Kim, J. Lee, and D. Sohn, *Bull. Korean Chem. Soc.*, **30**, 713 (2009).
- (15) S. Y. Chou, P. R. Krauss, and P. J. Renstrom, *Appl. Phys. Lett.*, **67**, 3114 (1996).
- (16) S. Y. Chou, P. R. Krauss, and P. J. Renstorm, *Science*, **272**, 85 (1996).
- (17) L. J. Guo, *Adv. Mater.*, **19**, 495 (2007).
- (18) D. Y. Khang, H. Kang, T. Kim, and H. H. Lee, *Nano Lett.*, **4**, 633 (2004).
- (19) J. Park, Y. S. Kim, and P. T. Hammond, *Nano Lett.*, **5**, 1347 (2005).
- (20) Y. Lu, X. Chen, W. Hu, N. Lu, J. Sun, and J. Shen, *Langmuir*, **23**, 3254 (2007).
- (21) M. Kim, K. Kim, N. Y. Lee, K. Shin, and Y. S. Kim, *Chem. Commun.*, **23**, 2237 (2007).
- (22) Y. Lee, S.-H. Park, K.-B. Kim, and J.-K. Lee, *Adv. Mater.*, **19**, 2330 (2007).
- (23) G. Y. Jung, Z. Y. Li, W. Wu, Y. Chen, D. L. Olynick, S. Y. Wang, W. M. Tong, and R. S. Williams, *Langmuir*, **21**, 1158 (2005).
- (24) H. Schiff, S. Saxer, S. Park, C. Padeste, U. Pieves, and J. Gorbrecht, *Nanotechnology*, **16**, S171 (2005).
- (25) L. Zhai, F. C. Cebeci, R. E. Cohen, and M. F. Rubner, *Nano Lett.*, **4**, 1349 (2004).
- (26) W. Chen, A. Y. Fadeev, M. C. Hsieh, D. Oner, J. Youngblood, and T. J. McCarthy, *Langmuir*, **15**, 3395 (1999).
- (27) G. R. J. Artus, J. Stefan, Z. Jan, H.-P. Gautschi, K. Marquarde, and S. Seeger, *Adv. Mater.*, **18**, 2758 (2006).